Kelvin-Froude wake patterns of a traveling pressure disturbance

Jonathan Colen[1] and Eugene B. Kolomeisky[2]
[1]*Department of Physics, University of Chicago, 5720 South Ellis Ave, Chicago, Illinois 60637, USA*
[2]*Department of Physics, University of Virginia, P. O. Box 400714, Charlottesville, Virginia 22904-4714, USA*
(Dated: October 13, 2018)

According to Kelvin, a point pressure source uniformly traveling over the surface of deep calm water leaves behind universal wake pattern confined within 39° sector and consisting of the so-called transverse and diverging wavefronts. Actual ship wakes somewhat differ in their appearance from both each other and Kelvin's prediction. The difference can be attributed to a deviation from the point source limit and for given shape of the disturbance quantified by the Froude number F. We show how Kelvin's argument can be modified to include finite-size effects and classify resulting wake patterns. For smooth pressure sources there exist two characteristic Froude numbers, F_1 and $F_2 > F_1$, such as the wake is only present if $F \gtrsim F_1$. For $F_1 \lesssim F \lesssim F_2$ the wake consists of transverse wavefronts confined within a sector of an angle smaller than Kelvin's. An additional 39° wake made of both transverse and diverging wavefronts is found outside the "transverse" sector for $F > F_2$. If the pressure source has sharp boundary, additional interference effects are present in the small Froude number limit.

PACS numbers: 47.35.Bb, 42.15.Dp, 92.10.Hm

It is impossible to overlook similarity of the wakes produced on deep water by objects as distinct in sizes, shapes and speeds as a waterfowl, a high-speed boat or a tanker. This property has its origin in hydrodynamic similarity of the flow pattern due to a point traveling pressure source discovered by Kelvin [1]. The conclusion is a consequence of linearity of the theory and the dispersion law of long gravity waves on deep water [2]

$$\omega^2(\mathbf{k}) = gk \tag{1}$$

where ω is the frequency of the wave of the wave vector $\mathbf{k}$, g is the free fall acceleration and $k = |\mathbf{k}|$. Indeed dimensional considerations imply that the flow pattern is only characterized by the acceleration g and the velocity of the source v that can be combined to form a single parameter of dimensionality of length,

$$l = \frac{v^2}{g}, \tag{2}$$

the Kelvin length, which has a physical meaning of the spatial scale of the wake. If the length is measured in Kelvin units (2), the problem of determining the wake pattern is parameter-free, i.e. all the wakes produced by point sources are geometrically similar (the proof of the statement is Eq.(7) below). The hallmark of the Kelvin wake drawn in Figure 1a is its "feathered" appearance due to the so-called transverse and diverging wavefronts confined within 39° sector [1–3].

The Kelvin wake is a dispersive counterpart of the Cherenkov and Mach wakes [4] produced by light and sound, respectively. In contrast to the latter, no threshold in the form of a requirement on the speed of the source is needed for its formation. Indeed, the wake behind a moving source is formed if there is a wave mode whose phase velocity ω/k matches the projection of the velocity of the source onto the direction of radiation. This statement known in marine hydrodynamics as the condition of stationarity [3] or in general physics context as the Cherenkov-Landau (CL) condition [4] applied to the dispersion law (1) acquires the form

$$\cos^2\theta = \frac{v^2}{gk} = \frac{1}{kl} \tag{3}$$

where θ is the angle between the direction of radiation of the gravity wave and the direction of motion of the source. Since $\cos^2\theta \leqslant 1$ the wake is present if the condition $kl \geqslant 1$ holds. Clearly for l fixed there always are modes that can participate in producing the wake.

Ship wakes observed in practice are not strictly similar. Indeed the wakes of tankers are significantly different in their appearance from the wakes of high-speed boats: the former are dominated by transverse waves while the latter are largely made of diverging waves. This is a consequence of finite size of pressure sources that Kelvin's solution neglects. For fixed shape these effects are captured by the Froude number F defined in terms of the ratio of the Kelvin length (2) to characteristic length scale a of the source (e.g. the hull length for a slender ship)

$$F = \sqrt{\frac{l}{a}} = \frac{v}{\sqrt{ga}}, \tag{4}$$

that also plays a central role in understanding the wave resistance [2, 3]. In marine practice applicability of the linear water wave theory [2] is limited by the effects of wave breaking which set an upper bound to the Froude number at $F \simeq 3$ that can be achieved by high-speed boats. We note that the Kelvin $a = 0$ limit corresponds to infinite Froude number, $F = \infty$, i .e. deviations from the ideal Kelvin wake seen in practice are not surprising.

The apparent wake angle is one of the most direct indicators of the wake pattern that can be measured,

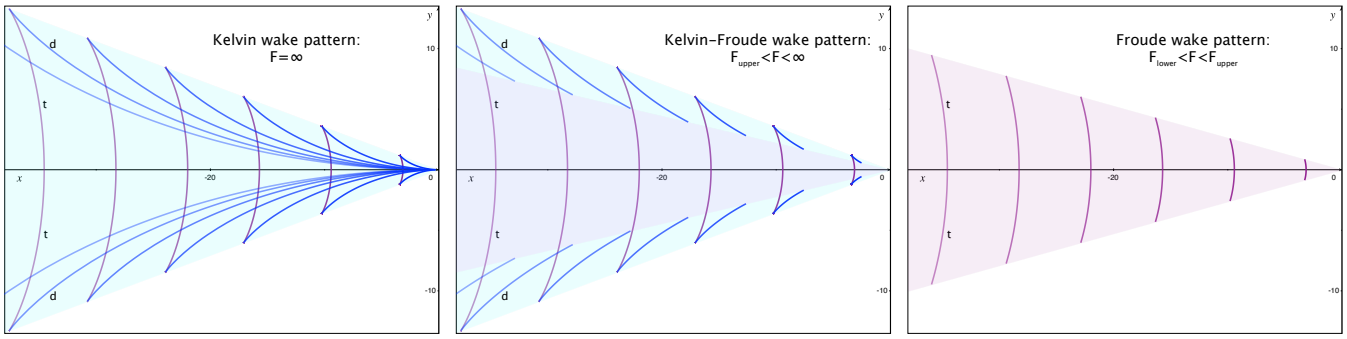

(a) (b) (c)

FIG. 1: (Color online) Evolution of the wavefronts due to the source at the origin traveling to the right, Eqs.(11) and (13), as functions of the cutoff parameter Q: (a) Kelvin wake, $Q = \infty$; (b) Kelvin-Froude wake, finite $Q > 3/2$, and (c) Kelvin-Froude wake, $1 < Q < 3/2$ in Kelvin units of length (2). Transverse (t) and diverging (d) wavefronts are shown in purple and blue, respectively. Regions where both transverse and diverging wavefronts are found are shaded light blue; regions with only transverse wavefronts present are shaded light purple. In cases (a) and (b) the entire wake is delimited by Kelvin's 39° angle. Opening angle of the sector with only transverse wavefronts present, cases (b) and (c), is given by Eq.(14).

and ship wakes narrower than Kelvin's have long been observed both in practice [5] and numerical studies [6]. The interest in appearance of ship wakes has recently been reignited following elegant study of Rabaud and Moisy (RM) [7] who inferred the dependence of the apparent angle of the wake on the Froude number F from a series of airborne images of ship wakes in the Google Earth database. The wake angle was found to be approximately constant and close to Kelvin's 39° prediction for $0.1 \lesssim F \lesssim 0.6$ while for larger Froude numbers the angle was decreasing with F reaching values as small as 14° at $F \simeq 1.7$ seemingly calling Kelvin's theory into question. RM's original explanation of these findings hinged upon an assumption that an object of size a cannot generate waves whose wavelength is larger than about a.

Recognizing that the apparent wake angle measured by RM corresponds to the locus of the peaks of highest waves, Darmon, Benzaquen, and Raphaël [8] provided an assumption free analysis of the observations [7] based on the classical linear water wave theory [2, 9] which was applied to the case of traveling isotropic Gaussian pressure source. The treatment also indicated that the entire wake was still delimited by Kelvin's 39° angle. Benzaquen, Darmon and Raphaël [10] further extended these ideas to understanding wake patterns and wave resistance due to anisotropic pressure disturbances more appropriate to the shapes of ships. Similar investigation has been carried out by Moisy and Rabaud [11]. Their interpretation however involved an assumption that amplitude of the waves excited by a disturbance of size a is small unless their wavelength is in a narrow band around a.

Rather different explanation of narrow wake angles due to Noblesse *et al.* [12] implemented classic idea of marine hydrodynamics [3] that the wake pattern of a ship can be understood as an interference of two opposite effect Kelvin wakes originating at the bow and stern of the ship. Central assumptions behind the three competing explanations of narrow wakes [7, 8, 10–12] have been critically assessed by He *et al.* [13].

These studies stimulated a series of fundamental questions regarding the gravity wake behind a ship that will be addressed in this work:

(i) What is the physics behind the wakes more narrow than Kelvin's? The assumptions regarding the relationship between the excited wavelength and the size of the source [7, 11] are controversial [13]. At the same time, the alternative assumption that the effect has largely a two-point interference origin [12], while physically plausible, has not been derived. Also geometric nature of the argument does not inform us of the magnitude of the effects in question.

(ii) Since there is more to the wake than apparent wake angle, how does the Froude number F control the appearance of the wake, i.e. what are possible wake patterns?

(iii) How is it possible for the wake to be delimited by Kelvin's 39° angle for F small ? It is a puzzle because in this case the pattern has to be least similar to the ideal, $F = \infty$, Kelvin wake.

Like in Refs.[8, 10] we begin with an expression for the vertical displacement of water surface due to a pressure source traveling with constant velocity $\mathbf{v}$ over deep water in the co-moving reference frame derived within the

framework of the linear water wave theory [2, 9],

$$\zeta(\mathbf{r}) = \frac{1}{\rho}\int \frac{d^2k}{(2\pi)^2}\frac{kp(\mathbf{k})e^{i\mathbf{k}\cdot\mathbf{r}}}{(\mathbf{k}\cdot\mathbf{v}+i0)^2-gk}, \tag{5}$$

where $\mathbf{r}$ is a two-dimensional position vector, ρ is the density of water and $p(\mathbf{k})$ is a Fourier transform of the excess pressure $\delta p(\mathbf{r})$ due to traveling disturbance,

$$p(\mathbf{k}) = \int \delta p(\mathbf{r}) e^{-i\mathbf{k}\cdot\mathbf{r}} d^2r. \tag{6}$$

The $+i0$ shift in the denominator of the integrand in (5) is required by causality [4]; it supplies a rule for bypassing the pole of the integrand.

Let us choose the positive x direction along the velocity vector $\mathbf{v}$, measure the length in Kelvin units (2), the wave vectors in units of l^{-1} and $\delta p(\mathbf{r})$ in units of $\rho g l$. Further specifying to the point source limit $p = const = 1$ brings the wake integral (5) to a parameter-free form

$$\zeta(\mathbf{r}) = \int \frac{d^2k}{(2\pi)^2}\frac{ke^{i\mathbf{k}\cdot\mathbf{r}}}{(k_x+i0)^2-k} \tag{7}$$

thus demonstrating geometric similarity of Kelvin wakes. Since the Kelvin limit continues to play central role for general $p(\mathbf{k})$ in (5), we begin with reviewing this case.

While the Fourier integral (7) cannot be computed in closed form, the geometry of the wake pattern can be understood by employing Kelvin's stationary phase argument [1–4]. First, the integral (7) is dominated by the wave vectors corresponding to the pole of the integrand

$$k_x^2 = k \tag{8}$$

which is the CL condition (3) in disguise. Second, far away from the source, $r \gg 1$, when the phase factor $f = \mathbf{k}\cdot\mathbf{r}$ in the integrand in (7) is large the exponential is highly oscillatory function of $\mathbf{k}$ so that contributions from various elements d^2k cancel each other; this is the case of destructive interference with almost zero net result. This cancelation, however, will not occur for the wave vectors satisfying the CL condition (8) for which additionally the phase f is stationary with respect to $\mathbf{k}$; this is the case of constructive interference.

The trace of the source divides the plane into two regions related to one another by reflection; without the loss of generality we can focus on the $y > 0$ half-space. Here the wake is formed by a superposition of the waves whose wave vectors have positive components, $k_{x,y} > 0$. Then the phase is given by

$$f = \mathbf{k}\cdot\mathbf{r} = \sqrt{k}\cdot x + \sqrt{k^2-k}\cdot y \tag{9}$$

where the components $k_{x,y}$ were expressed in terms of k according to Eq.(8). The condition of stationary phase $df/dk = 0$, i. e.

$$-\frac{y}{x} = \frac{\sqrt{k-1}}{2k-1} \tag{10}$$

can only be satisfied for $x < 0$ which is where the wake is. This relationship appeared previously [7]. The right-hand side of (10) vanishes at $k = 1$, $k \to \infty$, and for $k = 3/2$ it reaches a maximum value of $1/2\sqrt{2}$. Therefore the equation of stationary phase (10) has two solutions for $0 \leqslant -y/x < 1/2\sqrt{2}$ coalescing at $-y/x = 1/2\sqrt{2}$, and none for $-y/x > 1/2\sqrt{2}$. The locus of coalescence points lies on a ray that makes an $\arctan(1/2\sqrt{2}) \approx 19.47°$ angle with the negative x direction. This is Kelvin's classic result for the half-angle of the wake pattern [1].

Since the phase f is constant along the wavefront, Eqs.(9) and (10) can be solved relative to x and y to give the equation for the wavefront in parametric form:

$$x(k) = f\frac{2k-1}{k^{\frac{3}{2}}}, \quad y(k) = -f\frac{\sqrt{k-1}}{k^{\frac{3}{2}}} \tag{11}$$

Here the magnitude of the wave vector k plays a role of the variable parameter; internal consistency of the argument requires the phase to be negative, $f < 0$.

A series of these wavefronts is shown in Figure 1a where for the purpose of illustration we chose $f = -2\pi(n+1/2)$ with n integer; the $y < 0$ part of the wake is obtained by reflection. The wake consists of the transverse wavefronts formed by elementary waves with the wave vectors in the $1 < k < 3/2$ range connecting the edges of the pattern across the central line $y = 0$, and the diverging wavefronts formed by the waves with the wave vectors in the $k > 3/2$ range connecting the source at the origin to the edges of the pattern [1–3]. The wavelength of the pattern along the central line $y = 0$ is 2π while at the wake boundary $-y/x = 1/2\sqrt{2}$ it is $4\pi/3$ ($2\pi v^2/g$ and $4\pi v^2/3g$ in the original units of length, respectively).

Alternatively, the equation of the wavefront can be written out implicitly by substituting solutions of the equation of the stationary phase (10) into the expression for the phase (9):

$$f(x,y) = -\frac{x^2\left(1+4y^2/x^2 \pm \sqrt{1-8y^2/x^2}\right)^{3/2}}{4\sqrt{2}y(1\pm\sqrt{1-8y^2/x^2})} \tag{12}$$

and requiring that $f = const$. Here the upper and lower signs correspond to the diverging and transverse wavefronts, respectively; the entire wake is confined within a wedge delimited by the Kelvin rays $y/x = \pm 1/2\sqrt{2}$. We note that the phase function corresponding to the diverging wavefronts increases in magnitude without bound as one approaches the central line $y = 0$. This translates into oscillatory behavior of the water height with ever decreasing wavelength as $y \to 0$. This is the reason behind bunching of the diverging wavefronts in Figure 1a for y small. In practice such a behavior will be halted by a combination of the effects that present theory omits: capillarity neglected in the dispersion law (1) and nonlinearity that would come into play as a result of breakdown of potentiality of the flow inevitable for sufficiently

steep waves. While solution of this outstanding problem requiring additional physics ingredients will not be pursued in this work, finite-size effects, as will be made clear shortly, either eliminate this regime of behavior or push it to the domain of very large Froude numbers.

The effect of finite size and shape of pressure source on the wake pattern crucially depends on whether water surface piecing is absent or not. The former situation includes hovercraft, low-flying airplane or missile, or a boat in planing regime [3]. We will study it first as only modest modification of already given argument is needed for understanding.

This class of pressure sources can be described by smooth spatially localized excess pressure functions $\delta p(\mathbf{r})$ whose Fourier transforms $p(\mathbf{k})$ are localized in momentum space. The latter has an effect of imposing an ultraviolet cutoff in the integral (5), i.e. effective exclusion of large wave vector modes from participating in the interference of elementary waves. A simple way to account for this effect is to take a sharp cutoff approximation consisting in strict elimination of sufficiently large wave vectors from the integration domain in Eq.(7). Let Q be the magnitude of the wave vector that both satisfies the CL condition (8) and belongs to the boundary of the integration domain in (7): only the waves whose wave vectors satisfy the condition

$$k \in [1, Q] \tag{13}$$

now participate in producing the wake pattern. At this point we recall that the equation for the Kelvin wavefront (11) is given in terms of parametric dependences on the magnitude of the wave vector k. These equations subject to the constraint (13) also describe the wavefronts due to sharply localized pressure functions $p(\mathbf{k})$. All the information about the shape of the integration region in Eq.(7) is hidden in phenomenological parameter Q.

Evolution of the wavefronts (11) for different values of the cutoff parameter Q is shown in Figure 1. The Kelvin, $Q = \infty$ limit, Figure 1a, differs from the case of finite $Q > 3/2$, Figure 1b, in that the diverging wavefronts no longer reach the source at the origin. The locus of their end points defines an inner wake of the opening angle

$$\varphi_i = 2 \arctan \frac{\sqrt{Q-1}}{2Q-1} \tag{14}$$

that only consists of the transverse wavefronts; both diverging and transverse wavefronts are found outside the inner wake and are delimited by Kelvin's 39° angle. As Q approaches 3/2 from above, the inner wake widens and the segments of the diverging wavefronts decrease in length. At $Q = 3/2$ the inner wake angle (14) matches Kelvin's 39°, and the diverging wavefronts disappear. For $Q < 3/2$, Figure 1c, the wake consists entirely of the transverse wavefronts confined within the angle (14) smaller than Kelvin's. As the cutoff parameter Q approaches unity, the wake narrows and disappears for $Q < 1$. This fact could be anticipated by noticing that progressive elimination of the large wave vector modes achieved by decrease of the cutoff parameter Q inevitably comes into contradiction with the CL requirement $k > 1$. The absence of the wake for $Q < 1$ does not imply strict lack of the waves but rather an indicator that the stationary phase approximation no longer applies. The wakes having the appearance of those in Figures 1b or 1c that reflects finite-size effects are hereafter referred to as Kelvin-Froude wakes. It is curious that they resemble Kelvin-Mach wakes predicted to exist in two-dimensional electron systems [14] where the effect is due plasma waves whose dispersion law $\omega(\mathbf{k})$ deviates from the $k^{1/2}$ form (1) in an important way.

Sharply localized pressure functions $p(\mathbf{k})$ do not faithfully represent realistic pressure sources because their direct space counterparts $\delta p(\mathbf{r})$ feature decaying oscillatory behavior.

[1] L. Kelvin, Proc. Inst. Mech. Eng. 3, 409 (1887).

[2] H. Lamb, *Hydrodynamics* (6th ed., Cambridge University Press, 1975), Chapter IX.

[3] J. N. Newman, *Marine hydrodynamics* (Cambridge, Massachusetts, MIT Press, 1977), Chapter 6; see also Figures 6.16 and 6.17.

[4] I. Carusotto and G. Rousseaux, in *Analogue Gravity Phenomenology*, D. Faccio *et al.* (eds), Lecture Notes in Physics, Chapter 6, p.109, and references therein.

[5] D.W. Taylor, *Resistance of Ships and Screw Propulsion* (Macmillan, 1910); G.S. Baker, *Ship Form, Resistance and Screw Propulsion* (D. Van Nostrand Company, 1915); W. H. Munk, P. Scully-Power, F. Zachariasen, Proc. R. Soc. Lond. Ser. A **412**, 231(1987); D. Brown, S. B. Buchsbaum, R. E. Hall, J. P. Penhune, K. F. Schmitt, K. M. Watson, D.C. Wyatt, J. Fluid Mech. **204**, 263 (1989); A. M. Reed, J. H. Milgram, Ann. Rev. Fluid Mech. **34**, 469 (2002); M. C.Fang, R.Y. Yang, I. V. Shugan, J. Mech. **27**, 71(2011).

[6] F. Noblesse, *Analytical approximation for steady ship waves at low Froude numbers*, David W. Taylor Naval Ship Research and Development Center Report DTNSRDC-86/058 (1986); A. Barnell, and F. Noblesse, *Far-field features of the Kelvin wake*, in *Proc. 16th Symp. Naval Hydrodynamics* (National Academy Press, 1986) p.18-36; F. Noblesse and D. Hendrix, *Near-field nonlinearities and short far-field ship waves*, in *Proc. 18th Symp. Naval Hydrodynamics*, (National Academy Press, 1990), pp. 465-476.

[7] M. Rabaud and F. Moisy, Phys. Rev. Lett. **110**, 214503 (2013).

[8] A. Darmon, M. Benzaquen and E. Raphaël, J. Fluid Mech. **738**, R3 (2014); see also S. Å. Ellingsen, J. Fluid Mech. **742**, R2 (2014).

[9] T.H. Havelock, Proc. R. Soc. London A **95**, 354 (1919); E. Raphaël and P.-G. De Gennes, Phys. Rev. E **53**, 3448 (1996).

[10] M. Benzaquen, A. Darmon, and E.Raphaël, Phys. Fluids

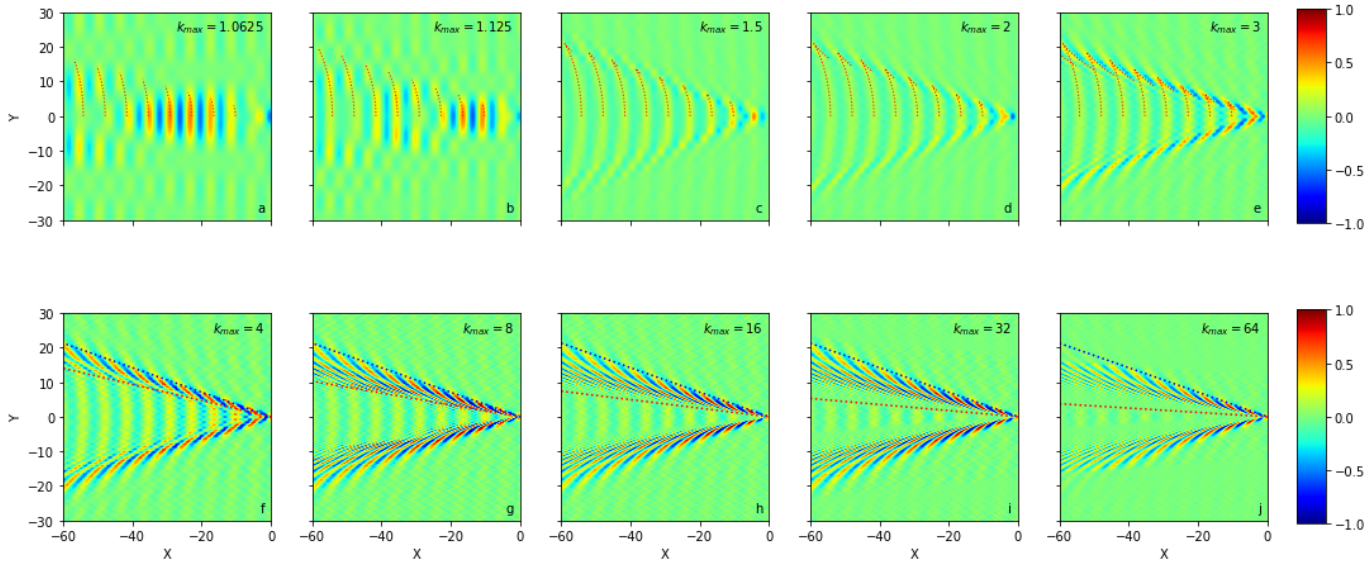

FIG. 2: (Color online)

26, 092106 (2014).

[11] F. Moisy and M. Rabaud, Phys. Rev. E **89**, 063004 (2014).

[12] F. Noblesse, J. He, Y. Zhu, L. Hong, C. Zhang, R. Zhu, and C. Yang, Eur. J. Mech. B/Fluids **46**, 164 (2014).

[13] J. He, C. Zhang, Y. Zhu, H. Wu, C.-J. Yang F. Noblesse, X. Gu and W. Li, Eur. J. Mech. B/Fluids **49**, 12 (2015).

[14] E. B. Kolomeisky and J. P. Straley, Phys. Rev. Lett. **120**, 226801 (2018).

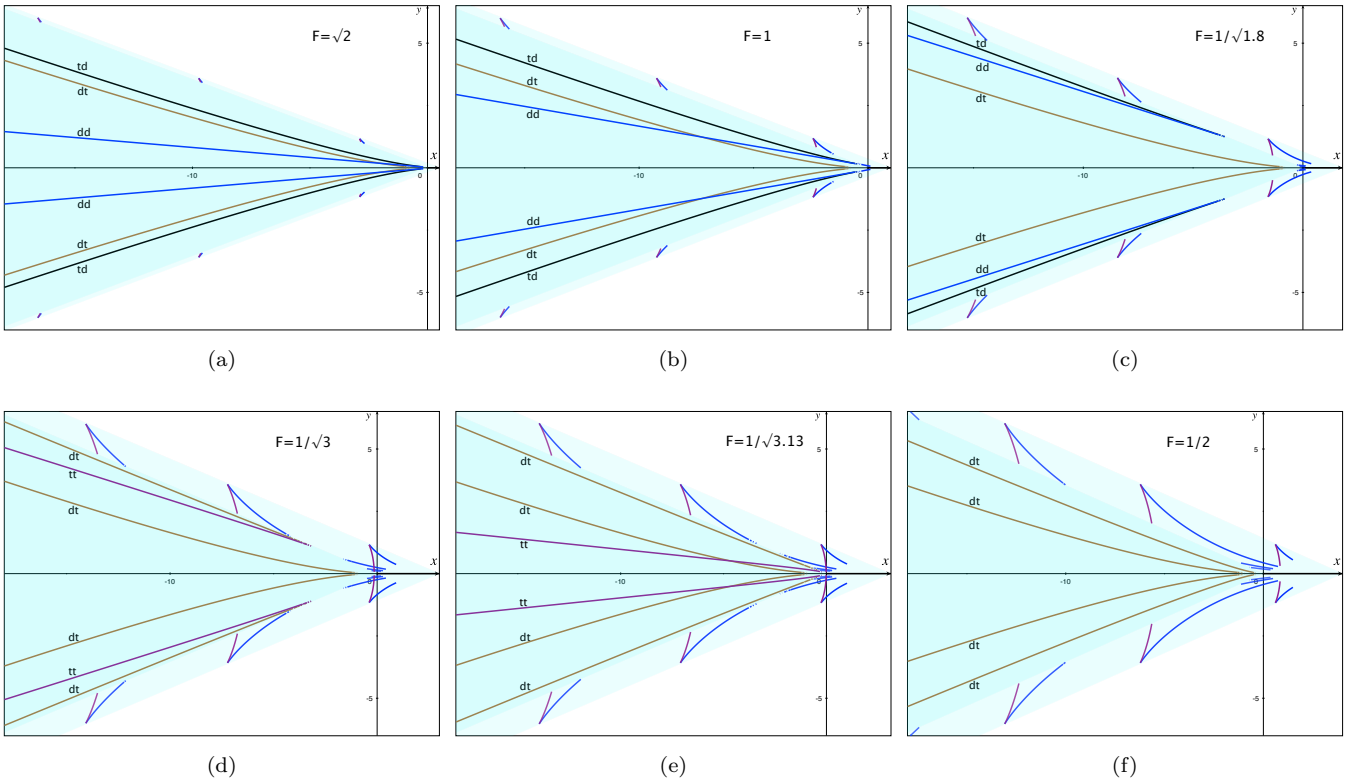

(a) (b) (c)

(d) (e) (f)

FIG. 3: (Color online) Linear pressure segment source.